The International Journal of Advanced Manufacturing Technology (2024) 130:5619–5626
https://doi.org/10.1007/s00170-024-13038-4

ORIGINAL ARTICLE

Hot-pressed calcium phosphates as a potential bone substitute: structural and mechanical characterization

Helena Pereira[1] · Oscar Carvalho[1,2] · Igor Bdikin[3] · Filipe Samuel Silva[1,2] · Georgina Miranda[4]

Received: 7 August 2023 / Accepted: 14 January 2024 / Published online: 25 January 2024

Abstract

The compositional similarity of calcium phosphates such as β-TCP and HAp to the inorganic components of human bones makes them excellent candidates for bone substitutes. Regardless of presenting excellent biocompatibility, calcium phosphates present low mechanical strength, which is a major drawback for load-bearing applications. In this sense, achieving Hap or β-TCP with increased density is crucial to enhance their mechanical properties. In the present study, β-TCP and HAp were processed from commercially available powders in order to obtain highly dense specimens aiming to elevate these mechanical properties of calcium phosphates. For this purpose, two sintering strategies were used: in the first, using a single holding time, whereas in the second, two holding times. The obtained phases, their potential degradation, microstructure, porosity, and mechanical strength were investigated. Results revealed that the use of two holding times improved densification, leading to flexural strength improvement, on both materials, but especially on HAp, where a 122% increase was verified.

Keywords Hydroxyapatite · Beta-tricalcium phosphate · Microstructure · Flexural strength · Density

1 Introduction

The increasing aging of the population and the rising numbers related to bone diseases, trauma, or fractures due to excessive mechanical loading and fatigue from repeated loading are pushing the need for long-lasting solutions for the orthopedic and dental fields [1, 2]. Although bone has an amazing capability to self-heal, when a defect exceeds the bone's capacity of self-regeneration, a graft is needed. Autografts are considered the optimal solution and are being used for several years; however, due to being an invasive and painful process, there is a growing interest in reducing their use [3, 4].

Since calcium phosphate–based bone substitutes have a chemical composition analogous to that of human bone and tooth enamel, they have been receiving research attention, additionally, besides being relatively easy to manufacture [5]. Even in the market, there is a diversity of calcium phosphate–based products available such as Graftys HBS [6] which is a mixture of α-tricalcium phosphate and dicalcium phosphate dehydrate, to mention a few, and Graftys Quickset which is made of calcium-deficient hydroxyapatite. Nevertheless, this products present low mechanical properties; for instance, Graftys Quickset has a compressive strength of 19.0 ± 2.5 MPa [7]. Hydroxyapatite ($Ca_{10}(PO_4)_6(OH)_2$; HAp) and beta-tricalcium phosphate ($Ca_3(PO_4)_2$; β-TCP) are the more studied calcium phosphate especially HAp which is analogous to the inorganic components of human bones, and therefore, it possesses properties that support osteoblast adhesion and proliferation, and new bone formation [8]. On the other hand, β-TCP is a brittle material which presents thermal stability range and, in addition to being osteoconductive and osteoinductive, it presents a cell-mediated resorption which makes it an interesting candidate for implants [9].

✉ Helena Pereira
helena.frs.pereira@gmail.com

1 Center for MicroElectroMechanical Systems (CMEMS), University of Minho (UMinho), Campus de Azurém, Guimarães, Portugal

2 LABBELS – Associate Laboratory, Guimarães, Braga, Portugal

3 Mechanical Engineering Department, TEMA, University of Aveiro, 3810-193 Aveiro, Portugal

4 Department of Materials and Ceramic Engineering, CICECO-Aveiro Institute of Materials, University of Aveiro, 3810-193 Aveiro, Portugal

While calcium phosphates have excellent biocompatibility, their low mechanical strength is still a major drawback for load-bearing applications. Therefore, achieving full dense structures of HAp or β-TCP is crucial to enhance their mechanical properties and using pressure-assisted techniques such as hot pressing (HP) or hot isostatic pressing (HIP) makes it possible as it leads to fine microstructures, higher density, and increased mechanical properties [10, 11]. These techniques apply simultaneous heat and pressure, yet in HIP process instead of uniaxial, the pressure is applied in three dimensions to the material [11, 12]. Furthermore, spark plasma sintering (SPS) technique is used as an alternative processing route once it reaches high levels of density nearly 99.6% for HAp specimens as reported in literature [13, 14].

The aim of this study is to fabricate highly dense HAp and β-TCP with improved mechanical properties by means of HP. For this purpose, two strategies were tested: the first was using a single holding time, but as the specimens, especially the HAp specimens, fracture frequently, another strategy was considered, which was based on two holding time in order to release any residual stresses. Surface characterization, as well as mechanical evaluation, was performed, and it was observed that the second led to an improvement on the mechanical properties, especially the flexural strength.

2 Materials and methods

2.1 HAp and β-TCP sintering

HAp with an average particle size of 2.5 µm (Fluidinova S.A., Portugal) and β-TCP with a particle size of 2.26 µm (Trans-Tech, USA), having a size distribution of d_{10} 0.69 µm, d_{50} 2.26 µm, and d_{90} 4.41 µm, were used to process cylindrical disc (10 mm in diameter and 2.4 mm in thickness). For the processing, a cylindrical graphite die (diameter 10 mm) coated by a thin film of boron nitride to prevent the diffusion between the die and the material was used.

Two different strategies were used in order to obtain full dense specimens with mechanical resistance. On the one hand, the powders were hot pressed for 30 min at 1100 °C in vacuum under a pressure of 40 MPa. The pressure was applied at 900 °C and kept constant until the holding temperature was reached; after the holding time, depressure was released due to the shrinkage avoiding the specimen breakage. Also, to prevent cracks in the processed discs, both heating rate and cooling rate were controlled. The heating rate was constant at 1.5 °C/s until 1100 °C. On the other hand, the cooling rate had two stages: a first stage until 300 °C was reached, having a cooling rate of 1.5 °C/s, and then the die was left to cool down naturally. This group will be named from now on as S1. In the second strategy, similar to the first strategy, the powders were hot pressed for 30 min at 1100 °C in vacuum under a pressure of 40 MPa; after the holding time, the pressure was released and the cooling rate was of 1.5 °C/s until 600 °C was reached and a second holding time of 30 min was performed. Finally, the die was cooled down at a rate of 1.5 °C/s until 300 °C was reached and then it was left to cool down naturally. After polishing, the second group of specimens underwent a thermal cycle of 700 °C during 2 h to release residual stress. This group will be named as S2 (Fig. 1).

2.2 Porosity measurements

Three specimens for each condition of the HAp and β-TCP discs were used for assessing the porosity. The apparent density was obtained by mass per unit volume of the sintered disc g/cm^3 [15]. The relative values were calculated, assuming, as a reference, 3.15 g/cm^3 for HAp and 3.07 g/cm^3 for β-TCP [15, 16]. The porosity of the sintered discs was determined using Eq. (1):

$$\text{Porosity}\ (\%) = 1 - \frac{\text{Weigth of sample}}{\text{Volume of sample} \times \text{Density of material}} \quad (1)$$

Also, Archimedes method was used to determine the bulk density of specimens by using deionized water as liquid medium.

2.3 Surface morphology

The S1 and S2 surface morphology was analyzed by scanning electron microscopy (SEM) to assess the presence of pores. Also, the grain size of the different groups was revealed on a mirror-polished surface followed by an acid etching (0.2 M citric acid) and the grain size was measured using the image software ImageJ. The sintered discs as well as the HAp and β-TCP powders were subjected to X-ray diffraction (XRD) phase analysis with 2θ range between 10 and 80° to assess the phase stability. For that purpose, a Bruker AXS D8 Discover (USA) was used and the obtained patterns were then compared to the JCPDS (Joint Committee on Powder Diffraction Standards) card using X'Pert HighScore Plus software for phase identification.

2.4 Evaluation of mechanical properties

2.4.1 Hardness test

In order to assess the mechanical properties of the calcium phosphate bulk discs produced in this study, experimental tests were performed. Microindentation tests were performed using

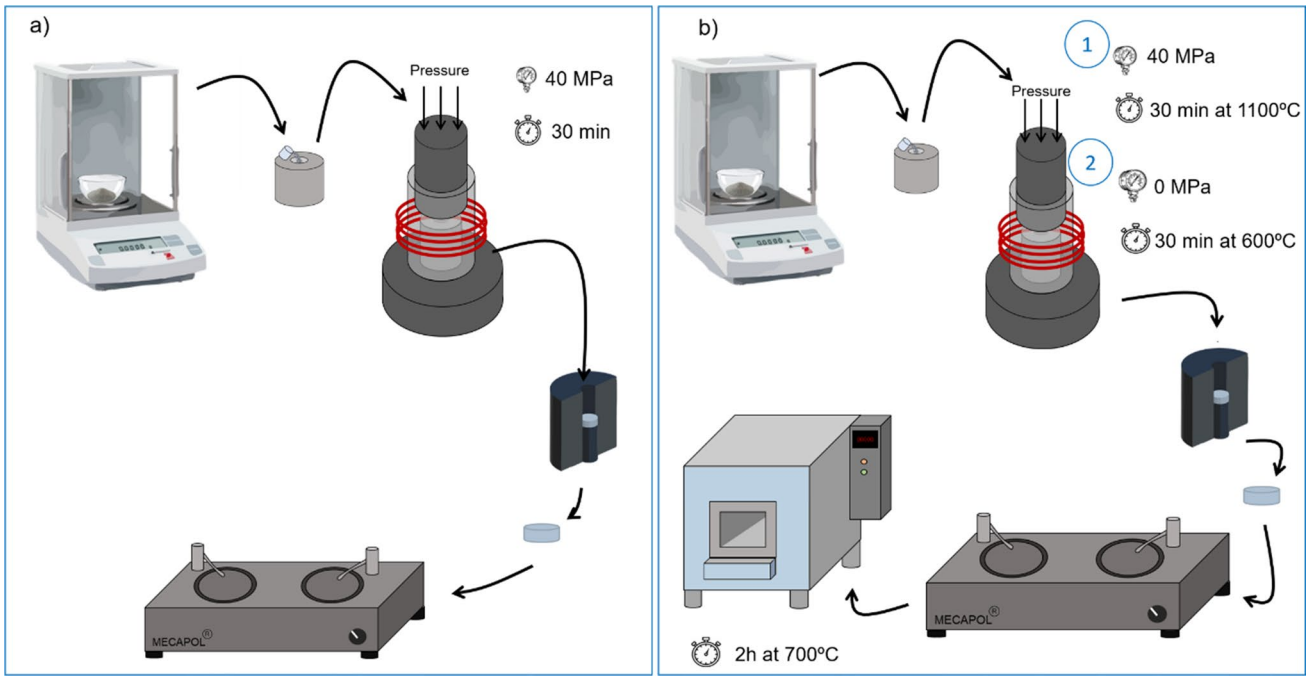

Fig. 1 Schematic representation of the fabrication strategies for the produced calcium phosphate specimens. **a** Strategy 1 (S1) group. **b** Strategy 2 (S2) group

three samples of each condition to calculate Vickers hardness (HV) of the sintered HAp and β-TCP discs, of both S1 and S2 groups. For this, DuraScan (EMCO-TEST) with a diamond indenter was used, and the hardness was calculated using Eq. (2) [17]:

$$\mathrm{HV} = \frac{1.8544L}{d^2} \tag{2}$$

where L (kgf) is the applied load and d (mm) is the average diagonal length of the indentation. By multiplying the hardness values obtained from Eq. (2) by the factor 0.009807, the values are converted to GPa. The indentation hardness (H_{IT}) and modulus (E_{IT}) were both obtained by nanoindentation using an instrumented indentation (TTX-NHT, CSM Instruments) using the Oliver–Pharr method [18]. This method allows to obtain more precise information about the material due to load and reload curves at different locations of the same sample [19]. The typical nanoindentation test consists in applying a force using loads ranging from 4 to 150 mN at a loading/unloading rate of 2 mN/min with a pause of 2 s at maximum force. The indenter used was a sharp Berkovich tip with a nominal edge radius of ~ 20 nm. The H_{IT} value was obtained using Eq. (3), and using Eq. (4), the E_{IT} was calculated.

$$H_{IT} = \frac{F_{max}}{A_p} \text{ in Pascal} \tag{3}$$

$$E_{IT} = \frac{1-\nu_s^2}{\frac{1}{E_r} - \frac{1-\nu_s^2}{E_i}} \tag{4}$$

where F_{max} is the maximum force (mN), E_i is the elastic modulus of the indenter, A_p is the projected contact area (mm^2), E_r is the reduced modulus of the indentation contact, V_i is Poisson's ratio of the indenter, and V_s is Poisson's ratio of the sample.

Prior to these tests, polishing was performed using MECAPOL P251 equipment using different types of sandpapers with different meshes, starting with P800 to P4000 grit size. Further polish was completed using a diamond suspension with a particle size of 3 µm (DiaPro Dur) followed by diamond suspension with a particle size of 1 µm.

2.4.2 Flexural strength test

The flexural strength of the HAp and β-TCP bulk discs was measured using the ball-on-three-balls test, and a custom-made stainless steel apparatus (Fig. 2) was made for this purpose in accordance with ASTM C1161. A servohydraulic machine (Instron 8874, MA, USA) equipped with a 25 kN load cell was used to perform the tests. Five samples of each material were tested at room temperature with a loading rate of 0.05 mm/s. During the test, the sample is in the holder where there are three steel balls placed evenly spaced from the center.

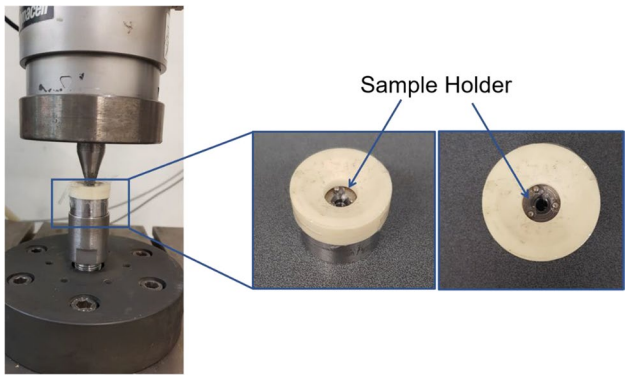

Fig. 2 Custom-made apparatus for the flexural strength tests

The fracture load was recorded, and the maximum tensile stress was calculated according to Eq. (5) [20, 21]:

$$\partial_{\max} = \frac{F}{t^2}\left[c_0 + \frac{c_1 + c_2\left(\frac{t}{R}\right) + c_3\left(\frac{t}{R}\right)^2 + c_4\left(\frac{t}{R}\right)^3}{1 + c_5(t/R)}\left(1 + c_6\frac{R}{R_a}\right)\right] \quad (5)$$

where F is the maximum force at fracture (N), t is the sample thickness (mm), R is the sample radius (mm), R_a is the support radius (4 mm), and the parameters c_0 to c_6 are dependent of Poisson's ratio of the different tested materials referring to fitting factors for the geometrical correction term, being $c_0 = -17{,}346$, $c_1 = 20{,}774$, $c_2 = 622.62$, $c_3 = 76.879$, $c_4 = 50.383$, $c_5 = 33.736$, and $c_6 = 0.0613$ the parameters used for HAp samples and $c_0 = -12.354$, $c_1 = 15.549$, $c_2 = 489.2$, $c_3 = -78.707$, $c_4 = 52.216$, $c_5 = 36.554$, and $c_6 = 0.082$ for β-TCP samples [21, 22].

3 Results and discussion

3.1 XRD analysis

A key aspect when processing bioactive ceramics like β-TCP and HAp at high temperatures is its crystalline structure after sintering, once it has been reported in literature that phase degradation can occur when high temperatures are used, especially above 1200 °C [23, 24]. In this sense, to determine the existing phases in the hot-pressed specimens of S1 and S2 groups, XRD analyses were performed and the resulting diffractograms are shown in Fig. 3. The XRD patterns of the as-received β-TCP and HAp powders are also present in Fig. 3. Main peaks of both β-TCP and HAp diffractograms match those determined for the base powder, revealing no phase transformation during the process. These results support that at a temperature of 1100 °C, no phase transformation occurs in β-TCP and HAp, on both S1 and S2 groups. Additionally, the peaks are in accordance with reference pattern numbers 003-0713 and 009-0432 for β-TCP and HAp, respectively. After the process, β-TCP and HAp phases

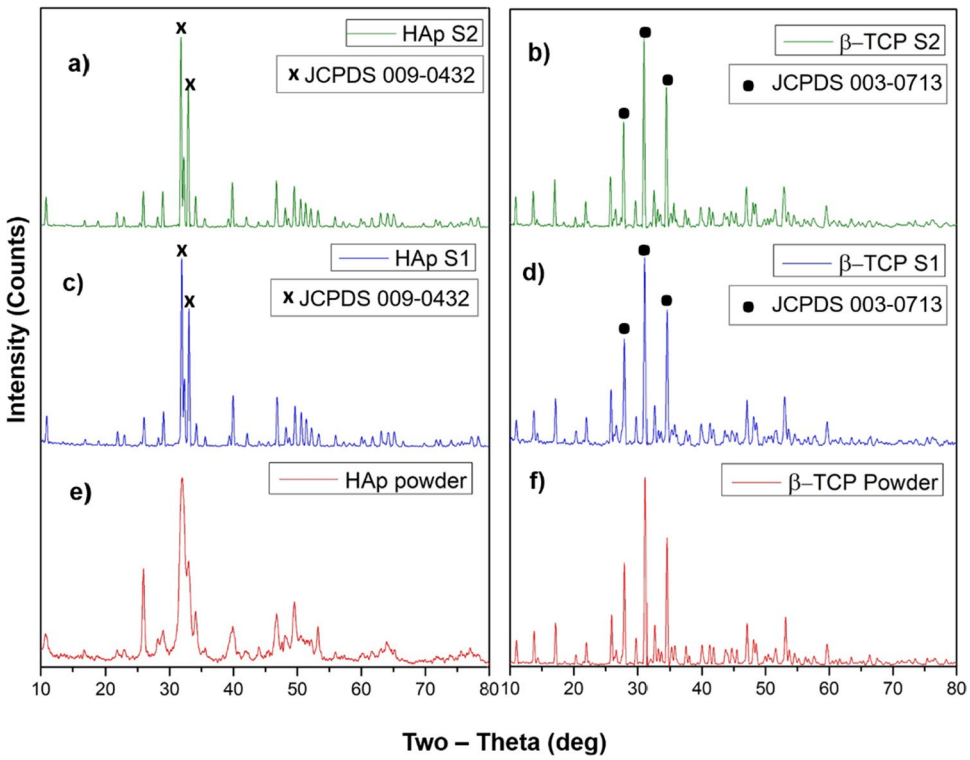

Fig. 3 X-ray diffraction patterns of calcium phosphate. **a** HAp of group S2. **b** β-TCP of group S2. **c** HAp of group S1. **d** β-TCP of group S1. **e** As received HAp powder. **f** As received β-TCP powder

in the samples are evident as it can be noticed by the increasing sharp reflections signaling the effect of crystal growth.

3.2 Porosity

The porosity was calculated by two different methods, by using Eq. (1) and by Archimedes methods being both results presented in Table 1. It can be concluded that the porosity of sintered samples was reduced with the addition of a second holding time of 30 min at 600 °C sintering temperature. The HAp density was 3.04 ± 0.03 g/cm^3 when one holding time was used and increased to 3.08 ± 0.06 g/cm^3 when the second holding time was added, leading to a superior densification than previously reported in literature [25, 26]. Regarding β-TCP results, a similar trend was observed with density increasing from 2.90 ± 0.02 to 2.96 ± 0.11 g/cm^3 when adding a second holding time, in line with previously reported by Descamps and colleagues [27].

3.3 SEM analysis

SEM analysis was used to evaluate β-TCP and HAp sinterability. Figure 4 gathers top views of SEM images for both S1 and S2 groups, and no visible porosity is identified, proving the effectiveness of the sintering at 1100 °C under 40 MPa. Additionally, the effects of hot pressing temperature on the microstructure of the different sintered specimens are perceived by analyzing the images in Fig. 4, where grain boundaries are visibly identified. Noteworthy in S2 group, the grain size increases from 1.93 ± 0.70 to 3.56 ± 1.79 µm with respect to β-TCP and from 2.24 ± 0.90 to 4.29 ± 0.95 µm with respect to HAp. It is perceived that by adding a second holding time, grain growth occurs for both materials which translate in the increasing of relative densities (Table 1). The obtained microstructure of the different hot-pressed specimens is well correlated with the measured density. Moreover, the density increase is an indicator of an improvement in mechanical properties.

Table 1 Density results for HAp and β-TCP S1 and S2 groups

Group	Specimen	Theoretical density (g/cm^3)	Archimedes density (g/cm^3)	Relative density (%)	Porosity
S1	β-TCP	2.90 ± 0.02	2.89 ± 0.100	94.48 ± 0.70	5.27 ± 0.69
	HAp	3.04 ± 0.03	2.99 ± 0.050	96.16 ± 0.95	3.84 ± 0.96
S2	β-TCP	2.96 ± 0.11	2.96 ± 0.100	99.1 ± 0.59	1.35 ± 0.32
	HAp	3.08 ± 0.06	3.01 ± 0.002	98.3 ± 0.05	2.36 ± 1.82

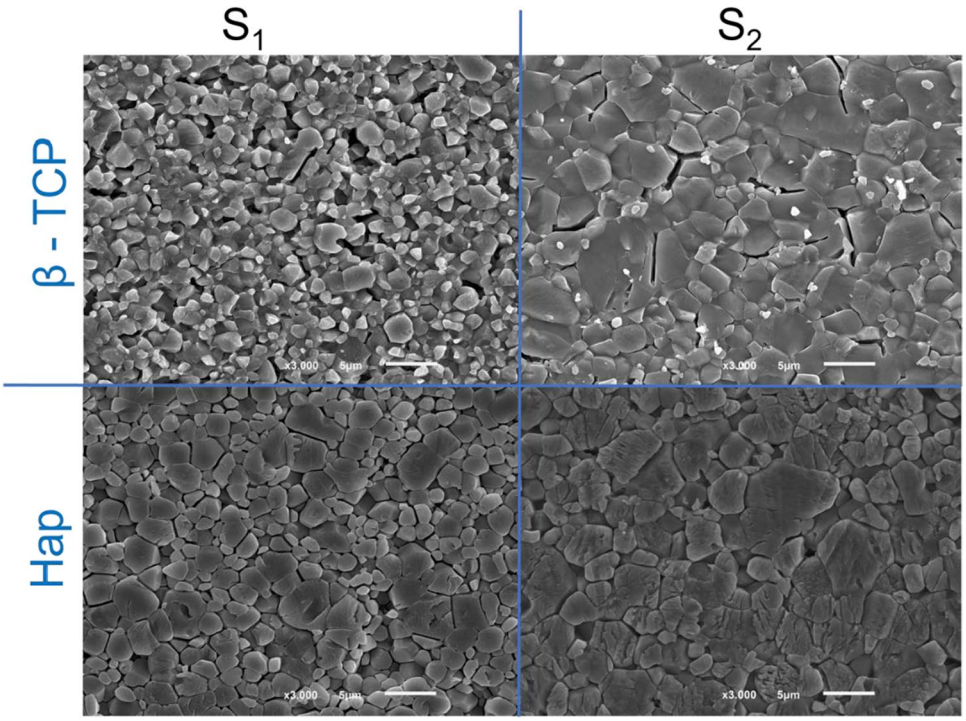

Fig. 4 HAp and β-TCP-polished surface for both S1 and S2 groups after acid etching

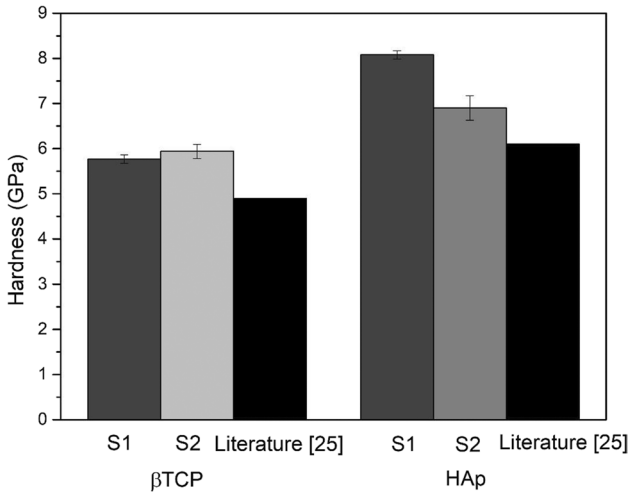

Fig. 5 Microindentation results for the different hot-pressed specimens (S1 and S2) and literature values [25]

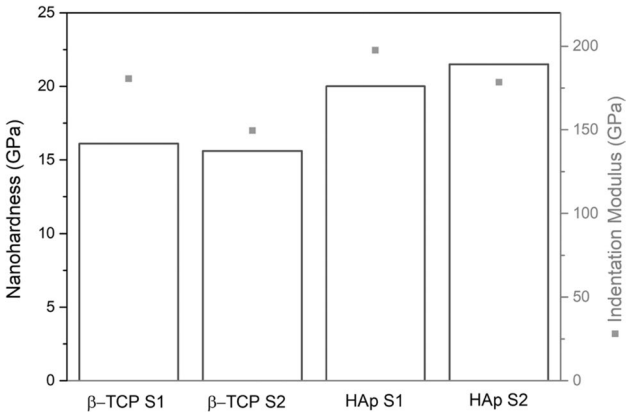

Fig. 6 Hardness and indentation modulus obtained from nanoindentation tests

3.4 Mechanical characterization

3.4.1 Microindentation

Figure 5 displays hardness results obtained from microindentation for HAp and β-TCP. Regarding HAp, a correlation between the grain size and the microhardness is perceived, with increasing grain size leading to a microhardness decrease, from 8.08 ± 0.092 GPa (S1, one holding time) to 6.9 ± 0.273 GPa (S2, two holding times). This tendency was previously reported for HAp in a study by Veljović et al. [26] where nanosized HAp powder was sintered and then hot pressed to obtain full dense HAp specimen. They observed that with increasing grain size, there was a decrease in microhardness. Regarding β-TCP, this tendency was not observed, once very similar hardness values were found for S1 and S2, which is in agreement with literature. A study by Tricoteaux et al. [28] observed that the increase of grain size in β-TCP leads to an increase in hardness.

3.4.2 Nanoindentation

The hardness and indentation modulus of the hot-pressed specimens of S1 and S2 groups were measured as a function of indentation depth (Fig. 6). Nanoindentation results allow evaluating two crucial parameters when developing bone substitutes: indentation hardness (H_{IT}) and indentation modulus (E_{IT}). The hardness of nanoindentation and microindentation depends on the grain structure and grain boundaries [26]. Samples have low porosity (Table 1), but numerous grain boundaries appear in grain structure (Fig. 5). Grain boundaries decrease the total hardness of the material since it is easier to destroy the grain boundary than the grain itself. Microindentation measurements involve more grains (and grain boundaries) for hardness analysis than nanoindentation. Thus, difference in absolute values for nanoindentation and microindentation can be explained by more local measurements in case of nanoindentation [29]. It can be perceived that β-TCP presents very similar nanohardness, in both S1 and S2, analogous to what we found for microhardness, whereas the HAp hardness increased from 20 to 21.4 GPa. Both β-TCP and HAp of group S2 presented lower indentation modulus than the corresponding S1 group (149.6 GPa and 178.5 GPa, respectively).

3.4.3 Flexural strength

The presence of pores, grain size, and grain boundaries has a great influence on the mechanical strength. Thus, a potential approach to improve the mechanical properties of these calcium phosphates is by obtaining high densification and fine microstructure. The values found in the literature are highly variable since different mechanical properties can be assessed and the variety of sample tested makes the comparison difficult [30].

Flexural strength is commonly assessed for these materials when thought for bone applications. Nevertheless, literature presents few flexural strength values for HAp and β-TCP and their majority results from HIP or SPS are related to composites gathering HAp and β-TCP [31–33].

Descamps et al. [27] reported, using HIP, that the flexural strength tends to decrease with the increase of HAp content. A similar tendency was observed in the present study for S1 group, where the obtained flexural strength was 25.66 ± 15.95 MPa for HAp (Table 2). Nevertheless, when adding the second holding time, the flexural strength improved to 56.9 ± 15.35 MPa which is directly related to the increase of density, from 2.99 ± 0.050 g/cm^3 (S1) to 3.01 ± 0.002 g/cm^3 (S2) (Table 2). Regarding β-TCP, the flexural strength difference between S1 and S2 groups is not considerable (52.25

Table 2 Flexural strength of the different groups (S1 and S2)

Group	Material	Flexural strength (MPa)
S1	HAp	25.66 ± 15.95
	β-TCP	52.25 ± 3.33
S2	HAp	56.9 ± 15.35
	β-TCP	53.9 ± 5.24

± 3.33 MPa (S1) and 53.9 ± 5.24 MPa (S2)), which is in accordance with the density results (2.89 ± 0.100 g/cm^3 (S1) and 2.96 ± 0.100 g/cm^3 (S2)). The difference concerning the flexural strength values of HAp and β-TCP on S2 group may be due to the different grain sizes, as β-TCP presents a variety of grain sizes throughout the surface (higher particle size distribution), while in the HAp, the grain size is more homogeneous. Ceramics with smaller grains are known to exhibit greater strength and hardness than those with larger grains because they offer more barriers against the progression of cracks [34].

4 Conclusions

In this study, dense β-TCP and HAp calcium phosphates were produced by hot pressing, leading to compacts with fully dense β-TCP and translucent HAp. The average grain sizes for S1 groups were 1.93 ± 0.70 μm with respect to β-TCP and 2.24 ± 0.90 μm with respect to HAp. For S2 group, an average grain size of 3.56 ± 1.79 μm and 4.29 ± 0.95 μm was obtained for β-TCP and HAp, respectively. The XRD analyses of the hot-pressed specimens proved no phase degradation, showing the effectiveness of the processing route.

The mechanical behavior of fully densified β-TCP and HAp calcium phosphates was studied. In general, the addition of a second holding time decreased the porosity and improved the flexural strength of both β-TCP and HAp. The maximum flexural strength was obtained for HAp fabricated using two holding time, being of 56.9 ± 15.35 MPa.

Acknowledgements This work was supported by FCT (Fundação para a Ciência e a Tecnologia) through the project PTDC/EME-EME/1442/2020 (Add2MechBio). This work was developed within the scope of the project CICECO-Aveiro Institute of Materials, UIDB/50011/2020, UIDP/50011/2020, and LA/P/0006/2020, financed by national funds through the FCT/MCTES (PIDDAC). Also, this work was supported by FCT national funds, under the national support to R&D unit grant, through the reference projects UIDB/04436/2020 and UIDP/04436/2020. Also, Helena Pereira acknowledges FCT for her PhD scholarship (2020.07257.BD). Igor Bdikin acknowledges the Portuguese Science Foundation (FCT) for the financial support of project CARBONCT (2022.03596.PTDC).

Author contributions Helena Pereira: formal analysis, methodology, investigation, and writing of original draft. Oscar Carvalho: conceptualization, methodology, writing which included review and editing, and supervision. Igor Bdikin: investigation and writing which included review and editing. Filipe Samuel Silva: project administration, funding acquisition, resources, and supervision investigation. Georgina Miranda: project administration, funding acquisition, resources, and supervision investigation.

Funding Open access funding provided by FCT|FCCN (b-on).

Declarations

Conflict of interest The authors declare no competing interests.

References

1. Fernandez de Grado G, Keller L, Idoux-Gillet Y, Wagner Q, Musset A-M, Benkirane-Jessel N, Bornert F, Offner D (2018) Bone substitutes: a review of their characteristics, clinical use, and perspectives for large bone defects management. J Tissue Eng 9:2041731418776819
2. Hernandez CJ (2013) Bone fatigue, stress fractures and bone repair (Sun Valley 2013). BoneKEy Rep 10:448
3. Schmidt AH (2021) Autologous bone graft: is it still the gold standard? Injury 52:S18–S22
4. Stahl A, Yang YP (2021) Regenerative approaches for the treatment of large bone defects. Tissue Eng Part B Rev 27(6):539–547
5. Samavedi S, Whittington AR, Goldstein AS (2013) Calcium phosphate ceramics in bone tissue engineering: a review of properties and their influence on cell behavior. Acta Biomater 9(9):8037–8045
6. Mellier C, Lefèvre F-X, Fayon F, Montouillout V, Despas C, Le Ferrec M, Boukhechba F, Walcarius A, Janvier P, Dutilleul M (2017) A straightforward approach to enhance the textural, mechanical and biological properties of injectable calcium phosphate apatitic cements (CPCs): CPC/blood composites, a comprehensive study. Acta Biomater 62:328–339
7. Brueckner T, Heilig P, Jordan MC, Paul MM, Blunk T, Meffert RH, Gbureck U, Hoelscher-Doht S (2019) Biomechanical evaluation of promising different bone substitutes in a clinically relevant test set-up. Materials 12(9):1364
8. Fihri A, Len C, Varma RS, Solhy A (2017) Hydroxyapatite: a review of syntheses, structure and applications in heterogeneous catalysis. Coord Chem Rev 347:48–76
9. Bohner M, Santoni BLG, Döbelin N (2020) β-Tricalcium phosphate for bone substitution: synthesis and properties. Acta Biomater 113:23–41
10. Dorozhkin SV (2013) Calcium orthophosphate-based bioceramics. Materials 6(9):3840–3942

11. Indurkar A, Choudhary R, Rubenis K, Locs J (2021) Advances in sintering techniques for calcium phosphates ceramics. Materials 14(20):6133
12. Singarapu B, Galusek D, Durán A, Pascual MJ (2020) Glass-ceramics processed by spark plasma sintering (SPS) for optical applications. Appl Sci 10(8):2791
13. Gu Y, Loh N, Khor K, Tor S, Cheang P (2002) Spark plasma sintering of hydroxyapatite powders. Biomaterials 23(1):37–43
14. Cuccu A, Montinaro S, Orru R, Cao G, Bellucci D, Sola A, Cannillo V (2015) Consolidation of different hydroxyapatite powders by SPS: optimization of the sintering conditions and characterization of the obtained bulk products. Ceram Int 41(1):725–736
15. Medvecky L, Stulajterova R, Giretova M, Sopcak T, Girman V (2022) Reinforcement of hydroxyapatite ceramics by soaking green samples of tetracalcium phosphate/monetite mixture in aqueous solutions. Ceram Int 48(12):17776–17788
16. Zhao Y, Sun K-N, Wang W-L, Wang Y-X, Sun X-L, Liang Y-J, Sun X-N, Chui P-F (2013) Microstructure and anisotropic mechanical properties of graphene nanoplatelet toughened biphasic calcium phosphate composite. Ceram Int 39(7):7627–7634
17. Sari Y, Saputra A, Bahtiar A, Nuzulia N (2021) Effects of microwave processing parameters on the properties of nanohydroxyapatite: structural, spectroscopic, hardness, and toxicity studies. Ceram Int 47(21):30061–30070
18. Oliver WC, Pharr GM (1992) An improved technique for determining hardness and elastic modulus using load and displacement sensing indentation experiments. J Mater Res 7(6):1564–1583
19. Shuman DJ, Costa AL, Andrade MS (2007) Calculating the elastic modulus from nanoindentation and microindentation reload curves. Mater Charact 58(4):380–389
20. Stares SL, Fredel MC, Greil P, Travitzky N (2013) Paper-derived hydroxyapatite. Ceram Int 39(6):7179–7183
21. Börger A, Supancic P, Danzer R (2004) The ball on three balls test for strength testing of brittle discs: part II: analysis of possible errors in the strength determination. J Eur Ceram Soc 24(10-11):2917–2928
22. Pabst W, Ticha G, Gregorová E (2004) Effective elastic properties of alumina-zirconia composite ceramics-part 3. Calculation of elastic moduli of polycrystalline alumina and zirconia from monocrystal data. Ceramics-Silikáty 48(2):41–48
23. Tecu C, Antoniac A, Goller G, Gok MG, Manole M, Mohan A, Moldovan H, Earar K (2018) The sintering behaviour and mechanical properties of hydroxyapatite-based composites for bone tissue regeneration. Rev Chim 69:1272–1275
24. Ishtiaque MS, Das H, Hoque SM, Choudhury S (2022) Synthesis of n-HAP using different precursors and dependence of Vickers hardness on the structure by tuning sintering temperature. Int J Appl Ceram Technol 19(3):1281–1292
25. Boilet L, Lardot V, Tricoteaux A, Leriche A, Cambier F, Descamps M (2023) Processing and properties of calcium phosphates bioceramics by hot isostatic pressing, vol 7. MATEC Web of Conferences, EDP Sciences, p 04020
26. Veljović D, Jokić B, Petrović R, Palcevskis E, Dindune A, Mihailescu IN, Janaćković D (2009) Processing of dense nanostructured HAP ceramics by sintering and hot pressing. Ceram Int 35(4):1407–1413
27. Descamps M, Boilet L, Moreau G, Tricoteaux A, Lu J, Leriche A, Lardot V, Cambier F (2013) Processing and properties of biphasic calcium phosphates bioceramics obtained by pressureless sintering and hot isostatic pressing. J Eur Ceram Soc 33(7):1263–1270
28. Tricoteaux A, Rguiti E, Chicot D, Boilet L, Descamps M, Leriche A, Lesage J (2011) Influence of porosity on the mechanical properties of microporous β-TCP bioceramics by usual and instrumented Vickers microindentation. J Eur Ceram Soc 31(8):1361–1369
29. Voyiadjis GZ, Yaghoobi M (2017) Review of nanoindentation size effect: experiments and atomistic simulation. Crystals 7(10):321
30. Johnson AJW, Herschler BA (2011) A review of the mechanical behavior of CaP and CaP/polymer composites for applications in bone replacement and repair. Acta Biomater 7(1):16–30
31. Veljović D, Zalite I, Palcevskis E, Smiciklas I, Petrović R, Janaćković D (2010) Microwave sintering of fine grained HAP and HAP/TCP bioceramics. Ceram Int 36(2):595–603
32. Ryu H-S, Hong KS, Lee J-K, Kim DJ, Lee JH, Chang B-S, Lee D-H, Lee C-K, Chung S-S (2004) Magnesia-doped HA/β-TCP ceramics and evaluation of their biocompatibility. Biomaterials 25(3):393–401
33. Raynaud S, Champion E, Lafon J, Bernache-Assollant D (2002) Calcium phosphate apatites with variable Ca/P atomic ratio III. Mechanical properties and degradation in solution of hot pressed ceramics. Biomaterials 23(4):1081–1089
34. Zilm M, Thomson SD, Wei M (2015) A comparative study of the sintering behavior of pure and manganese-substituted hydroxyapatite. Materials 8(9):6419–6436